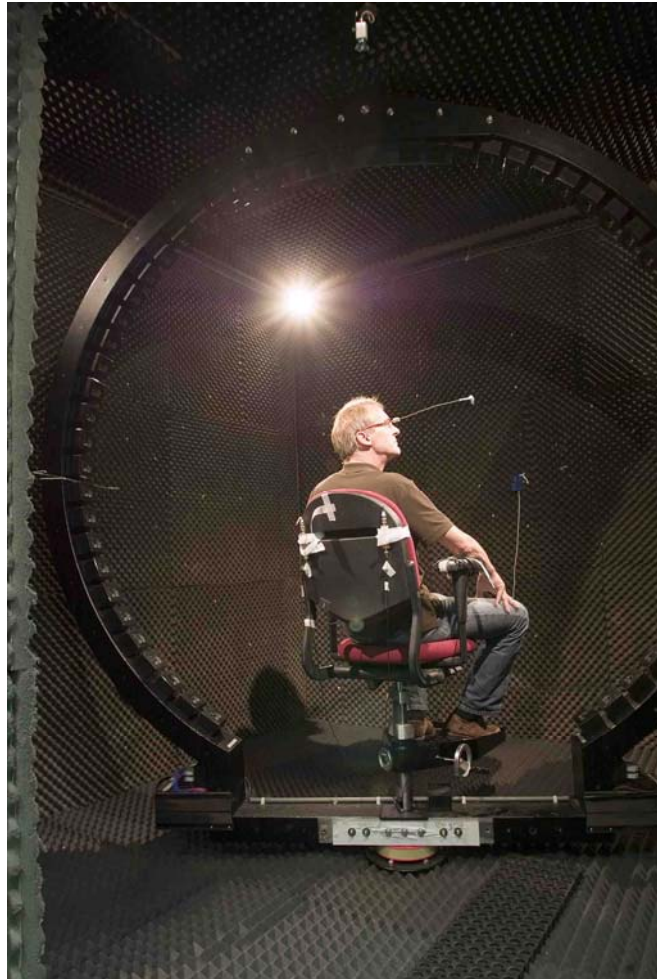


# 2010

Bachelorstage

Bart Alberts, Natuurwetenschappen  
o.l.v. Denise van Barneveld, Tom van  
Grootel en John van Opstal



## THE AUDITORY ZENITH: HOW AND WHERE?

This study describes the perception of the auditory zenith. Results show that subjects judged the auditory zenith accurately while sitting upright and sounds were presented in different planes. However, the precision in the front-back midsagittal plane through the head is dramatically decreased when compared to the frontal plane and intermediate planes. These results show that sounds in these intermediate planes are localized predominantly by binaural cues. When subjects have their heads rolled sideways, they estimated their head-centered auditory zenith accurately. Their world-centered auditory zenith, however, is shifted in the direction of head tilt. This is conform the Aubert effect in visual verticality perception, and is defined the auditory Aubert effect.

## *Table of Contents*

<b>General Introduction</b>	<b>3</b>
<b>Methods</b>	<b>11</b>
<b>Results</b>	<b>14</b>
<b>Discussion</b>	<b>18</b>
<b>Appendix A</b>	<b>20</b>
<b>Bibliography</b>	<b>23</b>

## 1 General Introduction

### Vestibular Cues

When a subject is in the dark, visual information is not available. This makes spatial orientation more challenging. However there are other sensory receptors available to detect our surroundings. In addition to senses like vision, hearing and touch, there are special receptors involved in detecting acceleration. Two types of acceleration are detected by the vestibular system. Linear acceleration, like gravity, is sensed by organs called the saccule and utricle, and the three semicircular canals detect angular acceleration, or head rotations. The human vestibular system protects us from feeling disoriented during head and body rotation, and they can provide motor commands to counter the effects of acceleration.

### Semicircular Canals

The semicircular canals are three fluid filled rings that lie on both sides of the head. They respond to angular acceleration around the axis normal to their plane (Highstein, 2004). In order to detect acceleration around every axis, the three canals are positioned approximately orthogonal to each other (figure 1.1B). Because the fluid inside the rings is of high viscosity, the hair cells inside the fluid will bend in a direction opposite to the rotation. Bending of the hair cells in one direction causes the cell membrane to depolarize, while bending in the opposite direction induces hyperpolarization. Depolarization is directly related to the firing rate of that cell. Whenever a rotation is sensed by the semicircular canals, one side of the head will have a higher firing rate, while the firing rate of the other side is reduced (figure 1.1A).

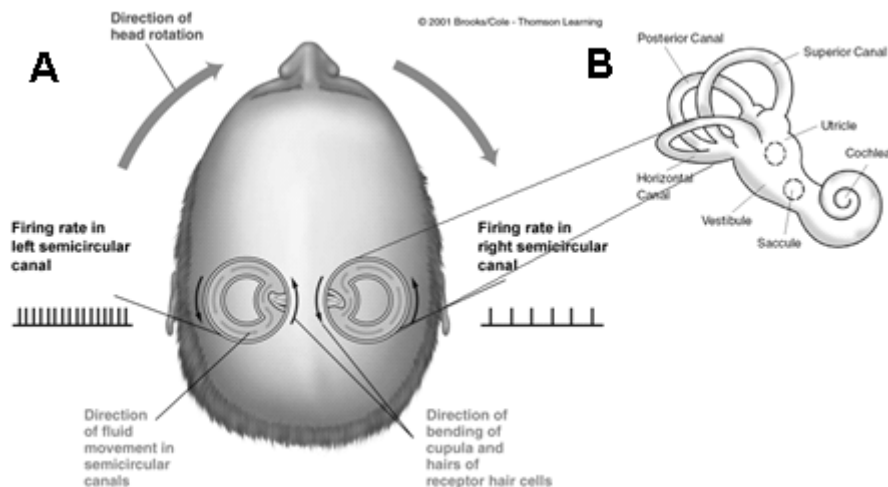


Figure 1.1. Schematic representation of the three semicircular canals. A) During head rotation, the canals on side of the head experience an increase in firing rate, while the canals on the other side of the head experience a decrease in firing rate. B) The three semicircular canals are positioned approximately orthogonal to each other. Adapted from Rhoades and Pflanzner, 2001.

### The Otoliths

The saccule and utricle are important sensors of the vestibular system detecting linear acceleration. Each saccule and utricle has a group of hair cells located in the horizontal and vertical planes. This group of hair cells is called the macula. On top of these macula lays a gelatin like membrane. Inside this membrane, there are granules consisting of calcium, called the otoliths. The pressure on the otolith changes due to changes in linear acceleration. This causes the cilia to displace providing a depolarizing current. Within each macula, the hair cells are orientated in two groups with

opposite directions (figure 1.2). Therefore, the otoliths are very sensitive for horizontal and vertical linear acceleration (Fernandez and Goldberg, 1976, Angelaki and Dickman, 2000).

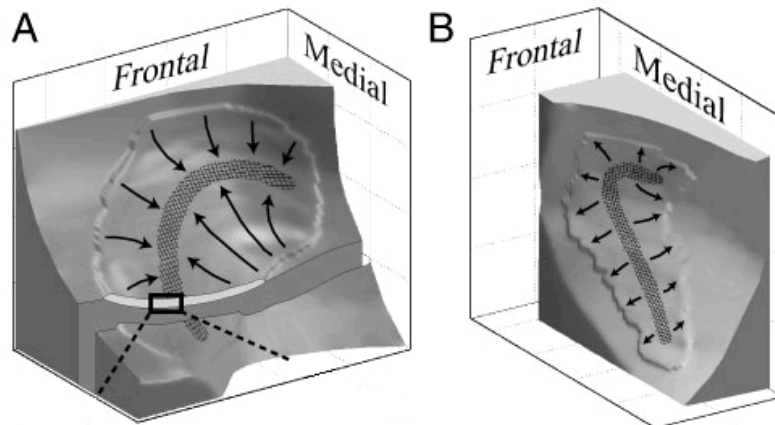


Figure 1.2. Three-dimensional curvature of utricle (A) and saccule (B). Arrow indicates local polarization direction of the hair cells. Inset shows the layers of the utricle: stiff Mesh layer and Gel layer. Adapted from Jaeger et al., 2002

### **Ambiguity problem**

As mentioned above, the inner ear possesses two accelerometers. However, Einstein (1908) pointed out that a signal from the otoliths is not enough to judge whether it arose from gravity or another linear acceleration or self motion. To deal with this ambiguity, neurons in the pons and midline cerebellum will produce an internal estimate of gravity using signals from the semicircular canals (Angelaki et al., 1999, Merfeld et al., 1999).

### **Subjective visual vertical (SVV)**

Kaptein and van Gisbergen (2004) showed that the percept of body tilt in the dark is perfect. This means that subjects are able to predict their body position in space from the vestibular and somatosensory cues available to the brain. However, when the subjects were tilted sideways (roll) and were asked to put a visual bar parallel to the earth's gravity vector, they showed systematic errors in visual verticality perception (figure 1.3A). Near upright, SVV errors are typically small (figure 1.3A and 1.4A), but at intermediate angles subjects experience overcompensation of verticality perception, known as the E-effect (figure 1.3A and 1.4B, Müller, 1916). At angles beyond 60 degrees subjects experience large undercompensation of verticality perception, known as the Aubert effect (A-effect, figure 1.3A and 1.4C, Aubert, 1861). In addition, De Vrijer et al 2008 showed that the uncertainty in positioning the bar vertical increases with tilt angle (figure 1.3B).

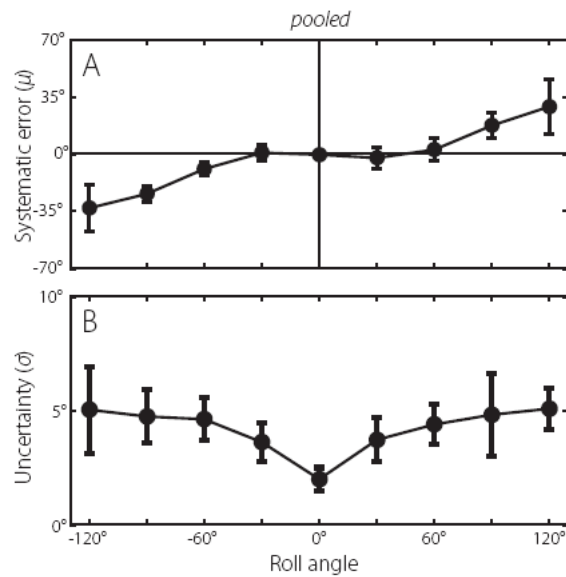


Figure 1.3. Pooled results from SVV task. A) Systematic errors, based on mean ( $\mu$ ) values  $\pm$  SD. B) Uncertainty, based on standard deviation ( $\sigma$ ) values  $\pm$  SD versus head tilt angle, averaged across subjects. Adapted from De Vrijer et al., 2008.

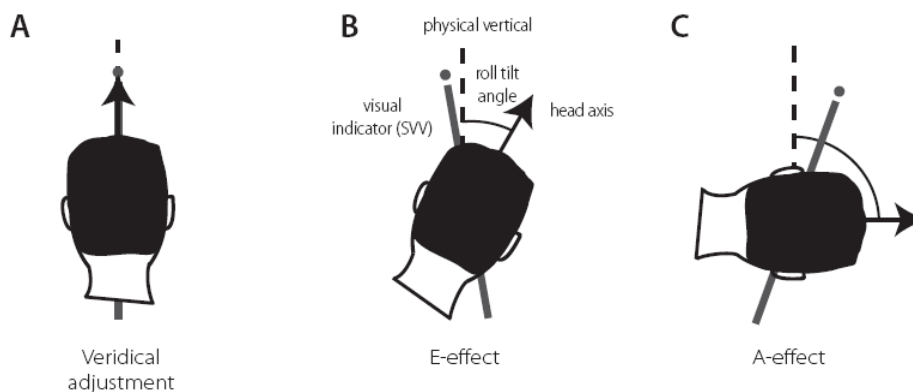


Figure 1.4. Schematic representation of SVV errors. A) Perfect verticality perception at zero tilt. B) Overcompensation (E-effect) at intermediate angles. C) Undercompensation (A-effect) at large angles. Adapted from De Vrijer et al., 2010.

### A-effect explained by head-fixed bias

Mittelstaedt (1983) explained this result as a compromise between a gravicentric signal (estimate of direction of gravity  $G$ ) and a head-fixed bias signal ( $M$ ) called the idiotropic vector (figure 1.5). The idiotropic vector is added vectorially to the estimated direction of gravity derived from the otoliths. This addition biases the tilt estimate towards the head axis, compensating for the E-effect, but enhancing the A-effect. Note that the gravicentric signal is not directly aligned with the direction of gravity because of the imperfect fusion of utricle and saccule information. This is because there are more cells in the utricle than in the saccule.

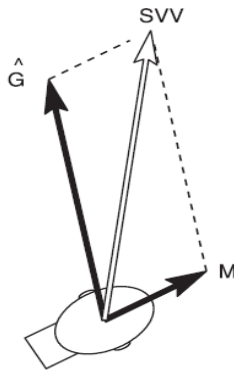


Figure 1.5. Schematic representation of Mittelsteadt's explanation of the subjective visual vertical (SVV). The idiotropic vector (M) biases the gravicentric signal of the otoliths (G) towards the head axis. Adapted from Mittelsteadt (1983)

### A-effect explained by Bayesian model

A recent explanation of the Aubert effect is given by De Vrijer et al. (2008). They propose a Bayesian model to explain the interaction of body tilt and subjective verticality, with two inputs from the outside world (figure 1.6). Their model is based on the summation of the target information in eye coordinates ( $T_E$ ) with the head position in space ( $H_S$ ) obtaining the target information in space ( $T_S$ ). The eye position in the head ( $E_H$ ) is kept zero.

$$T_S = T_E + E_H + H_S \quad (1)$$

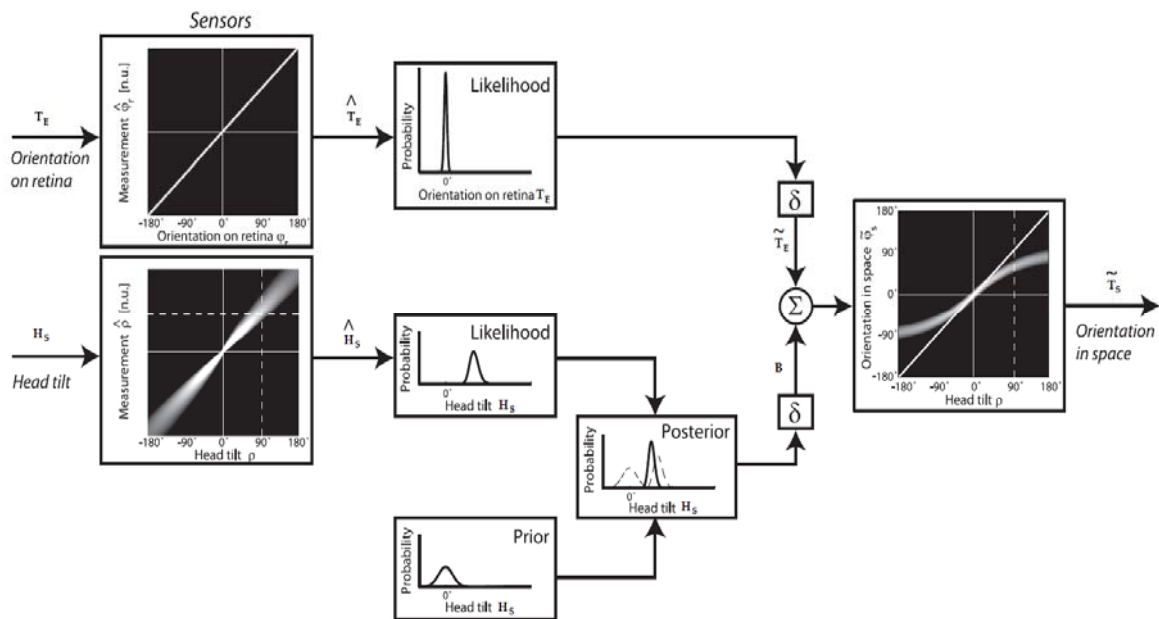


Figure 1.6. Schematic representation of Bayesian model explaining the undercompensation of visual verticality perception at angles beyond 60 degrees. The visual information on the retina  $T_E$ , is assumed to be encoded perfectly, resulting in a narrow likelihood distribution  $\hat{T}_E$ . The head tilt signal  $H_S$  is encoded by the otoliths and contaminated with noise which increases with larger tilt angle. This results in a broad likelihood distribution  $\hat{H}_S$  which is centered on the tilt angle  $H_S$  (in this example 90 degrees). The brain assumes a more likely head tilt, which is centered on zero degrees, and does not depend on the tilt angle. Bayes rule states that the posterior distribution is the multiplication of the prior and likelihood distribution resulting in a sharper, but biased distribution with respect to the likelihood distribution. A decision rule selects the compensatory angle  $B$  with maximum probability (MAP,  $\delta$  box). In the top line the brain selects the orientation  $\hat{T}_E$  with the maximum probability. A linear combination of both the visual orientation on the retina and the head orientation

in space results in the target orientation in space  $\hat{T}_s$ . Adapted from De Vrijer et al., 2008.

In the top left corner the primary input, the visual information, is fed into the model. It represents how a light bar is projected on the retina. This visual information is assumed to be encoded perfectly. This is seen as a narrow peak in the likelihood distribution. The narrow peak is close to a perfect delta function. The second input, the sensory head tilt of the subject, is encoded by the otoliths in the vestibular system. This signal is assumed to be accurate, but contaminated with noise, which increases with larger tilt angle.

Besides these two sensory signals, the brain is believed to use prior knowledge about head position. It assumes that the head being upright is more likely than it being tilted. This can be modeled in a prior distribution that has a peak at zero degrees (figure 1.6 bottom). Bayes rule (Dayan and Abbott, 2001) states that multiplication of the prior distribution  $P(H_s)$  and the likelihood distribution  $P(\hat{H}_s | H_s)$  results in a posterior distribution (figure 1.7).

$$P(H_s | \hat{H}_s) = P(\hat{H}_s | H_s)P(H_s) \quad (2)$$

This posterior distribution of this model is sharper than the likelihood distribution, which means it is more *precise*. Nevertheless, the prior induces also a bias with respect to the likelihood function, making the posterior distribution less *accurate* than the likelihood function.

Subsequently, a decision rule is imposed to select the compensatory angle for the head tilt (B in figure 1.6) with the maximum probability (MAP). Since the prior visual information is assumed to be flat, the observer selects the orientation of the likelihood function with the maximum probability. A linear combination of the compensatory tilt angle and the visual orientation with maximum probability results in the target representation in space.

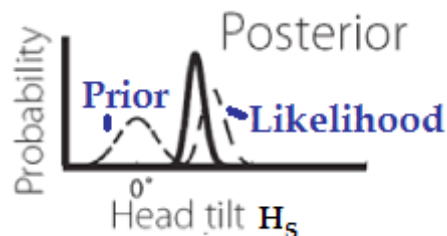


Figure 1.7. Schematic representation of Bayes rule. Multiplication of the likelihood function and prior distribution (dashed lines) result in a sharper, but biased posterior distribution with respect to the likelihood function.

## Auditory Cues

The question is if this model still applies in other sensory environments. In our study we focus on auditory stimuli, which are sensed not as precise as the visual information by the retina. In contrast to visual cues, auditory cues do not have explicit spatial cues, but spatial perception is constructed by implicit cues. These implicit cues are time difference, level difference and spectral cues.

### **Interaural Time Difference (ITD)**

For humans, relevant sound frequencies lie between 20 Hz and 20000 Hz. This means a wavelength of about 17.5 m for low pitches and about 1.75 cm for very high pitches. Because the distance between the two ears is about 15 cm, low pitches can easily bend around the head, up to including pitches of about 20-25 cm wavelength (1500-2000 Hz). Because there is an interaural distance, this immediately creates an interaural time difference (ITD). Depending on the location of the source, sound will enter one ear later than the other. Note that this does not hold for sounds coming from straight ahead. In this situation, the distance from sound to ear will be the same for both ears.

The information enters the mammalian auditory system at the Medial Superior Olive (MSO, Jeffress, 1948). The characteristics of this brain area are shown in figure 1.8A. One MSO cell gets information from both Cochlear Nuclei (AVCN) and thus from both ears. If only one signal arrives, the MSO cell will not give an output. Only if there is a signal from both the left and right side at the same time, there will be an output. The nerves from the CN towards the MSO cell differ in length. This means that whenever the interaural time difference is being compensated by the time difference in the nerves, the MSO fires an action potential. The brain processes the information of nerve length and constructs a source location.



Figure 1.8A. Brain pathway of the interaural time differences, which are encoded in the Medial Superior Olive. Adapted from Van Opstal, <http://www.mbfys.ru.nl/~johnvo/localisatie/itd2.html>.

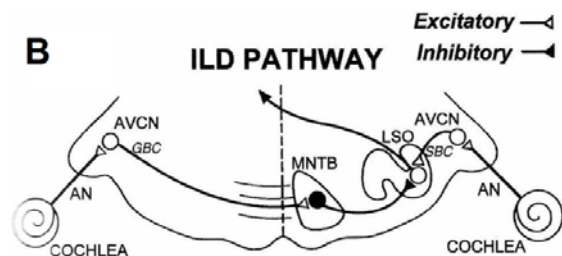


Figure 1.8B. Brain pathway of the interaural level differences, which are encoded in the Lateral Superior Olive. Adapted from Van Opstal, <http://www.mbfys.ru.nl/~johnvo/localisatie/ild2.html>.

Sounds which consist of high frequencies cannot be localized by interaural time difference. The distance between the ears is larger than the wave length of high frequencies. This means that several periods of the wave fit into the distance between the ears. The MSO cannot distinguish between one or several periods having passed already.

### **Interaural Level Difference (ILD)**

At high frequencies the head becomes a significant obstacle for sound waves, creating an intensity difference between both ears, known as the interaural level difference (ILD). The mammalian auditory system processes the intensity information in the Lateral Superior Olive (LSO, figure 1.8B, Tollin, 2003). Cells in the LSO are activated by sounds from the ear on the same side (ipsilateral) and are inhibited by sounds from the other ear (contralateral). This simple subtraction



will give the intensity difference between the two ears. The LSO passes its information also to the contralateral side of the brain. As for the ITD pathway, the ILD pathway is being processed for every sound frequency.

### Spectral cues

The mechanisms explained above are only relevant for sources in the horizontal plane (azimuth). In the 3D world, there are numerous of locations that will give the same ITD's and ILD's. Because the sound location with equal ITDs and ILDs lay on a cone shape, this phenomenon is called the cone of confusion (Blauert, 1997). There has to be another mechanism to solve this problem and detect the location of a source.

This third localization cue is the spectral cue and works differently from the mechanism of ILD and ITD. Where ILD's and ITD's are dependent on both ears (binaural cues), spectral cues only use information from one ear (monaural cues). The main characteristic of spectral cues is the spectrum of the sound which depends on the location and composition of the source (Middlebrooks and Green, 1991). Before the sound will reach the eardrum, the pinna attenuates and amplifies specific pitches. When sound waves hit the pinna, a part of the sound energy will be transferred inside, but a lot will first reflect at the different protrusions before reaching the ear canal. A reflected wave will enter the ear canal later than a direct wave (compare figure 1.9's dashed lines and solid lines). In the ear canal, the direct wave and the indirect waves add up. Because the pinna is asymmetric, this travel distance difference is strongly dependent on elevation of the source (figure 1.9). Therefore the ear functions as an elevation dependent filter. The pinna of every human is different, so the spectrum of the elevation angle plotted against the frequencies is called an ear print (figure 1.10), named after the fingerprint because it is also individual and different among humans. The brain uses a learned representation of the ear print as a theoretical look-up table to judge where the sound source is located.

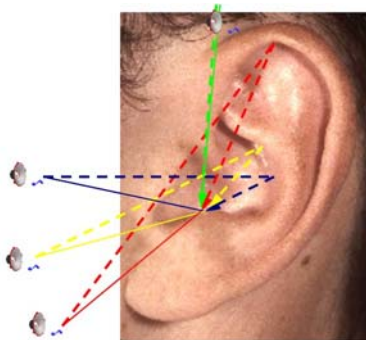


Figure 1.9. Reflection of sound waves at the pinna. Notice that orientation of the source is important. Both figure 1.9 and 1.10 are adapted from Van Opstal, <http://www.mbfys.ru.nl/~johnvo/localisatie/oorschelp2.html>

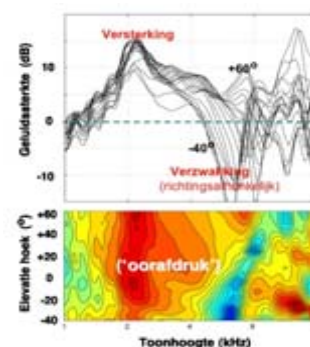


Figure 1.10. A human ear print. At the top the enhancement of the frequencies is plotted at every elevation angle. Underneath a contour plot shows the areas which are enhanced and reduced.

### Estimate of Auditory Zenith

Because the auditory cues are not assumed to be encoded perfectly in the brain, the likelihood distribution in the model of De Vrijer (figure 1.6,  $\hat{T}_E$ ) will be broader for sounds. The question is, if the described model also holds for auditory stimuli. A possible explanation is that the visual sensory input in the original model is considered with a sharp likelihood and a flat prior. The question is whether the model can still use a linear combination of auditory information and the information of head tilt, or that the model needs adjustment.

In this study we tested subjects on sound location judgments around the auditory zenith. The auditory zenith is the point straight above the head when sitting upright. On top of the subject's head we can define two planes, which are two divergent situations of hearing (figure 1.11). In the frontal plane (FP) the subject predominantly has to rely on binaural cues, whereas in the midsagittal plane (MSP) the subject can only rely on spectral cues. When the head is tilted in the FP (head roll, see figure 1.12), the sound location percept can change along two extremes or along an intermediate frame of reference. The perceived location can move with the head rotation (head-fixed) or can stay fixed relative to space (earth-fixed).

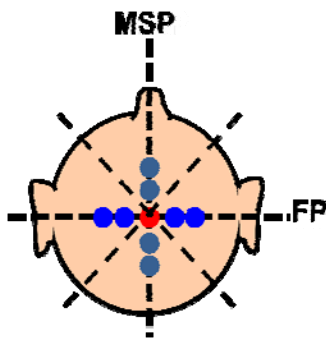


Figure 1.11. Sound locations around the auditory zenith. Sounds are presented in the frontal plane (FP), midsagittal plane (MSP) and two intermediate orientations (45 and -45 degrees) when sitting upright.

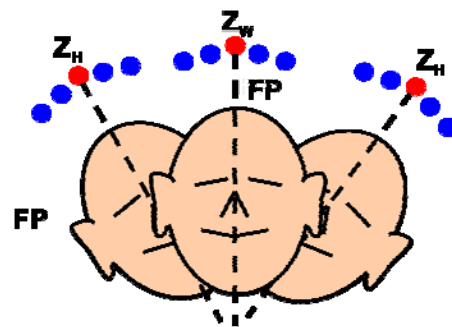


Figure 1.12. During head tilt, the perceived sound location can move with the head rotation ( $Z_H$ ) or stay fixed relative to space ( $Z_W$ )

We try to gather evidence about the sound localization system and how it behaves during head roll and whether we can extend the model of De Vrijer (figure 1.6, 2008) to auditory localization as well.

Our research questions are:

- Can we predict the resolution of all intermediate orientations from the two extreme situations (FP and MSP) of hearing? What is the influence of head roll on the auditory zenith?
- Is the perceived auditory zenith in the head-fixed reference frame or in the earth-fixed reference frame or in an intermediate reference frame?

## 2 *Methods*

### **Subjects**

Four subjects (all male) were tested, including the author. Subjects, aged between 20 and 22 years, were free from known vestibular or other neurological disorders and had no hearing deficiency.

### **Setup**

#### **Experimental setup**

Subjects were seated in a completely dark, sound-attenuated, anechoic room, in which a hoop with 58 speakers attached could move around the subject (figure 2.1). The speakers are located with 5 degrees spacing in elevation. Because the 29 speakers on the front half of the hoop were offset by 2.5 degrees to those on the back half of the hoop, an elevation resolution of 2.5 degrees was created. The resolution in azimuth was well below one degree. Three orthogonal magnetic fields were constructed by three pairs of squared coils in the corners of the room. The magnetic fields induced alternating voltages in the dual search coil mounted on the subject's head in order to record head position. This dual coil consists of a direction coil and a torsion coil that are located perpendicular to each other. The direction coil is located in the frontal plane, whereas the torsion coil is located in the perpendicular midsagittal plane. The torsion coil has the shape of an eight-figure in order to cancel the flux measured in the frontal plane. In Appendix A, an experimental protocol is proposed, which allows one to determine the absolute 3D orientation of the dual search coil. Apart from coil signals, two buttons on a button box were recorded. The signals were digitized at a rate of 1017.25 Hz/channel.



Figure 2.1. Experimental setup. Anechoic, sound-attenuated room, which contains a hoop with 58 speakers attached. Three orthogonal magnetic fields in the corners of the room induce alternating voltages in the dual search coil mounted on the subject's head.

### Stimuli

The sound used in the experiments was 150ms of Gaussian White Noise (cutoff frequencies: 20Hz HP and 20kHz LP) with an intensity of 60dBA (measured at subject's head with a Brüel and Kjaer microphone B&K 3134 and measuring amplifier B&K 2610). Sound could be played from a single location with a resolution of 5 degrees with a stationary hoop. However, by varying the intensity of two neighboring speakers, a higher resolution could be achieved (Serway, 2004). For a spherical sound source, the intensity in radial direction as a function of the distance  $r$  from the center of the sound source is:

$$I(r) = \frac{P}{4\pi r^2} \quad (3)$$

in which  $P$  is the actual power of the source. Because all the speakers are attached to a hoop, the distance  $r$  is the same for every speaker, making the sound waves of two different speakers constructive. This means that the sound level intensity increases with 6 dB when two speakers with the same intensity are played. To account for this intensity increase, the speaker intensity  $L_{dB}$  is:

$$L_{dB} = 60dB - \frac{3dB}{1 - R_{int}} \quad (4)$$

in which 60 dB is the intensity measured at subject's head, and  $R_{int}$  is the ratio between the two sound level intensities. When both intensities are the same,  $R_{int}$  is 0.5, making the speaker intensity of both speakers 54 dB. When the intensity of one speaker is set to zero and the other is set to 1, the intensities are set manually to 0 dB and 60 dB respectively because this equation cannot account for an intensity ratio of 1.

In Matlab, the speakers are controlled by a level function  $L_{SP}$ , that has a saturation intensity and a noise offset intensity and is proportional to the sound level intensity  $L_{dB}$ :

$$L_{SP} = (L_{dB} - 47) * 0.0085 + 0.88 \quad (5)$$

### **Experimental Paradigm**

Subjects were required to respond in a two alternative forced choice approach. Subjects responded by pressing either one of two buttons on a button box, to indicate whether the sound was perceived to the left or right in a FP stimulus configuration or front or back in MSP configuration. In a subsequent experimental block, subjects were required to indicate whether the sound was perceived left or right of the **head axis** in a FP configuration during head roll. This experiment was repeated once again, but now subjects had to indicate whether the sound was left or right of the **gravity axis** in a FP configuration.

### **Upright position**

In a baseline experiment, the subject was sitting upright and sounds were presented sounds in the frontal, midsagittal plane and two intermediate orientations (-45 and 45 degrees, figure 2.2). In the FP, sounds were presented between 7.5 degrees left to the head axis (negative angles) and 7.5 degrees right to the head axis (positive angles) with a resolution of 2.5 degrees by varying the intensity of two neighboring speakers (equation 4). Close to the auditory zenith (smaller than 2.5 degrees) resolution was further decreased to 1.25 degrees. In the MSP, sounds were presented between 40 degrees behind the head axis (negative angles) and 40 degrees in front of the head axis (positive angles) with a resolution of 5 degrees close to the head axis (smaller than 20 degrees) and 10 degrees else. In both intermediate orientations sounds were presented between 12.5 degrees (right-front or left-front) and -12.5 degrees (left-back or right-back) with a resolution of 2.5 degrees close to the head axis (smaller than 7.5 degrees) and 5 degrees else.

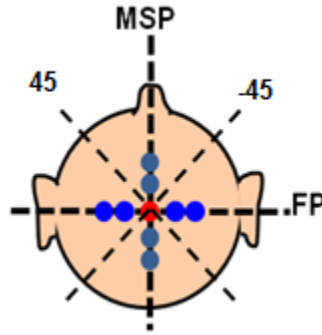


Figure 2.2. Sound locations around the auditory zenith when sitting upright. Sounds are presented in the frontal plane (FP), midsagittal plane (MSP) and two intermediate orientations.

### Head roll

In both experiments including head roll, the head was tilted to 35 degrees (right ear down) and -35 degrees (left ear down, figure 2.3). When subjects had to indicate whether the sound was left or right of the head axis, sounds were presented between 7.5 degrees left of the head axis and 7.5 degrees right of the head axis ( $\pm 35$  degrees) with a resolution of 1.25 degrees close to the head axis and 2.5 degrees else. When subjects were required to indicate whether the sound was left or right of the gravity axis during -35 degrees head roll, sounds were presented between 10 degrees right of the gravity axis and 40 degrees left of the gravity axis with a resolution of 5 degrees. The same experiment was performed during head roll of 35 degrees.

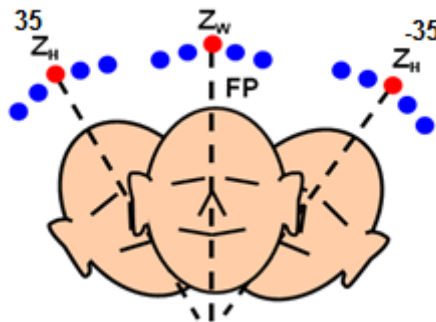


Figure 2.3. Subject's tasks during head roll of 35 degrees right ear down or 35 degrees left ear down. Subjects had to respond whether the sound was left or right of the head axis  $Z_H$  or left or right of the gravity axis  $Z_w$ .

### Data Analysis

Data analysis was performed off-line using Matlab software (Matlab 7.6, Mathworks). Psychometric data from the experiments were analyzed in a customary manner. We calculated the proportion of correct responses for each stimulus location and fitted a cumulative Gaussian curve using the method of maximum likelihood (Wichmann and Hill, 2001). This curve  $\psi(x)$  is given by

$$\psi(x) = \lambda + (1 - 2\lambda) \frac{1}{\sigma\sqrt{2\pi}} \int_{-\infty}^x \exp\left(-\frac{(\gamma - \mu)^2}{\sigma^2}\right) d\gamma \quad (6)$$

in which  $x$  is the location of the stimulus and  $\gamma$  an integration variable that runs over all stimuli. The mean value  $\mu$  represents the subject's subjective vertical, which serves as a measure of the subject's *accuracy*. The slope in the curve  $\sigma$ , represents the noise in the subjective vertical, which serves as a measure of the subject's *precision*. The lapse parameter  $\lambda$ , represents stimulus independent errors caused by mistakes of subjects for example. This parameter is allowed to be maximally 10%.

### 3 Results

We investigated in these experiments how *accurate* and *precise* subjects are in determining the location of auditory zenith. Next to this, we investigated the ability of subjects to compensate for static head tilt, when their task was to predict whether the sound was left or right of the head axis or left or right of the gravity axis.

#### The auditory zenith when sitting upright

Figure 3.1 shows the individual results of subject RB when sitting upright for all four stimulus configurations. The thresholds of the psychometric curves in figure 3.1 indicate that the subject is *accurate* in determining the location of the auditory zenith in all four configurations. The slopes are an indication of the *precision* of the subject. The results on the precision of predicting the auditory zenith differ between the four conditions. Slopes of the intermediate orientations are closer to the slope of the psychometric curve in the FP than in the MSP. Furthermore, the slope of the MSP configuration is close to zero.

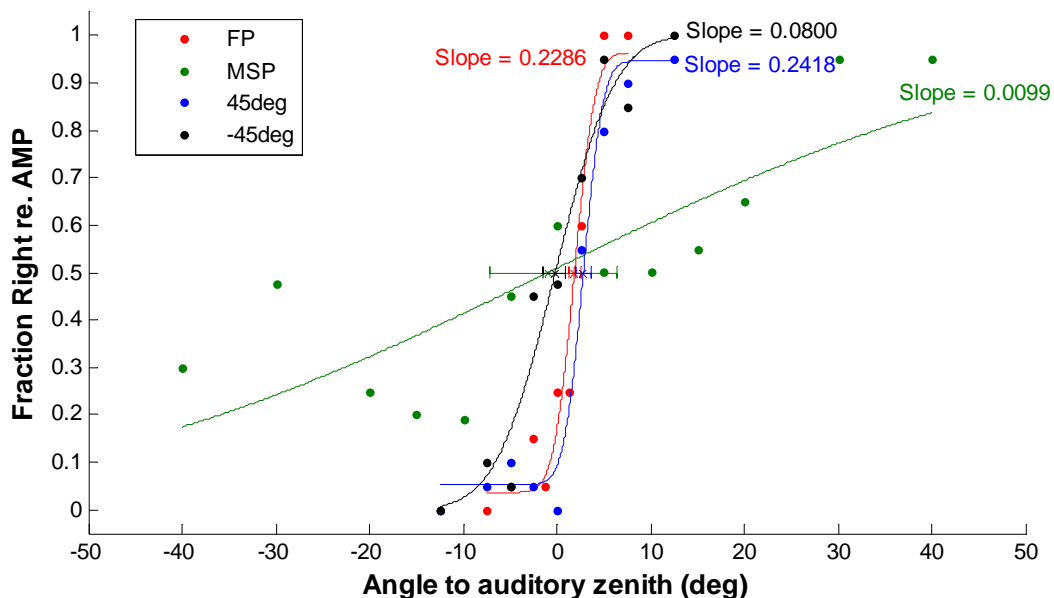


Figure 3.1. Subject RB: Psychometric curves of frontal plane (FP), midsagittal plane (MSP) and two intermediate orientations. Where the threshold of the curves is representative for the *accuracy* of the subject, the slope is representative for the *precision* of the subject.

Figure 3.2A and 3.2B show the results of all four subjects on the *accuracy* and *precision* of predicting the auditory zenith. In figure 3.2A, the thresholds of all configurations are within five degrees of the head/gravity axis (0 degrees), except for the MSP condition of subject BA. This threshold is about 30 degrees to the left of the head axis, because the responses of the subject in this configuration were completely random. This data thus could not be fitted reliably by a Cumulative Gaussian. The main trend in this figure is that all subjects are accurate in defining where the auditory zenith is located.

In figure 3.2B, the slopes of all curves are shown. The intermediate orientations have a slope close to the slope of the FP condition, whereas the MSP configuration slope is close to zero. In the FP configuration subjects can only rely on binaural cues, while subjects can only rely on monaural cues in the MSP. This means that the monaural cues around the auditory zenith are poorly defined, resulting in a poor *precision*. The precision in the frontal plane and intermediate orientations is better, meaning that subjects rely mostly on binaural cues in intermediate orientations.

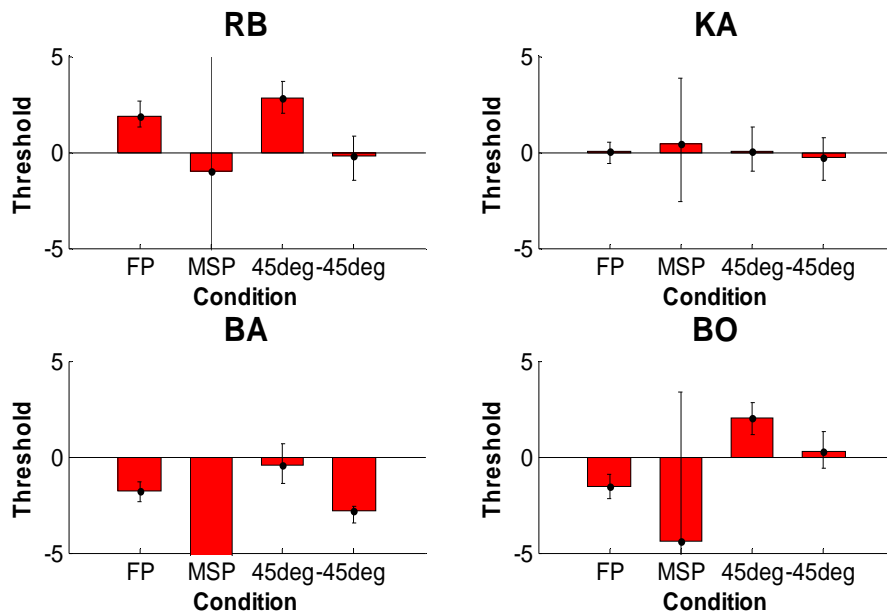


Figure 3.2A Subject's accuracy defined as the threshold of the psychometric curves. All thresholds are within 5 degrees of the auditory zenith, except for the MSP of subject BA. This is because the responses in the MSP of this subject were completely random. The results show that all four subjects are accurate in determining where the auditory zenith is located.

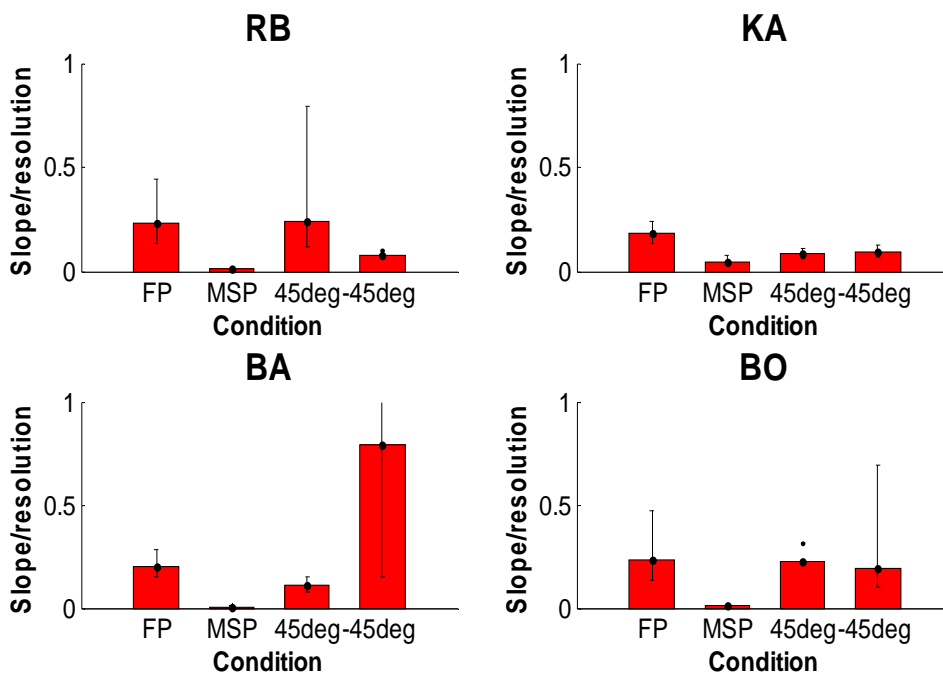


Figure 3.2B Subject's precision defined as the slope of the psychometric curves. Slopes of the intermediate orientations are close to slope of FP configuration, whereas the slopes of the MSP configuration are close to zero. Results indicate poor precision in MSP and that the intermediate orientation are as precise as the FP configuration.

### Compensation for body tilt is incomplete

The results of the task to determine whether a sound was left or right of the head axis during head roll of  $\pm 35$  degrees are shown in figure 3.3A for subject RB. The threshold in both curves is close to the head axis, meaning that the subject is *accurate* in determining where the auditory zenith is located when the head is tilted  $\pm 35$  degrees.



Figure 3.3B shows the results of subject RB for determining whether the sound was left or right of the gravity axis during head roll of  $\pm 35$  degrees. The threshold in these two curves is not aligned with the gravity axis (0 deg), making the subject *inaccurate* in compensating for body tilt when the auditory zenith has to be aligned with the gravity axis.

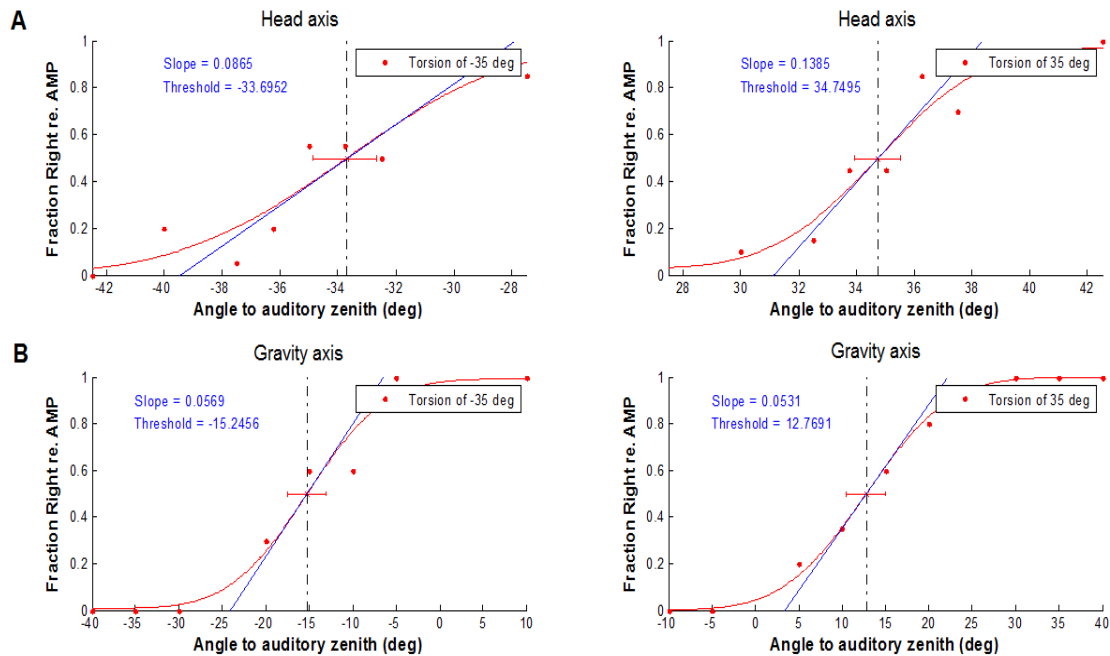


Figure 3.3. A: Psychometric curves of subject RB when the task was to determine whether the sound was left or right of the head axis during head roll of 35 degrees. Subject is accurate in predicting where the head axis is. B: Psychometric curves of subject RB when the task was to determine whether the sound was left or right of the gravity axis during head roll of 35 degrees. Subject is not accurate in predicting where the gravity axis is located.

### Accuracy

Figure 3.4 shows the thresholds of the psychometric curves of all subjects. In figure 3.4A the accuracy of aligning the auditory zenith with the head axis is shown, whereas figure 3.4B shows the accuracy of aligning the auditory zenith with the gravity axis. The dashed lines in figure 3.4A show the expected locations of the head axis. All subjects are able to align the auditory zenith with the head axis *accurately*. However, if the subjects have to align the auditory zenith with the gravity axis, errors between 10 to 30 degrees are made. This means that subjects have incomplete head tilt compensation, creating a bias in determining the exact location of the gravity axis. This result is conform the results of Kaptein and Van Gisbergen (2004) on visual vertical perception.

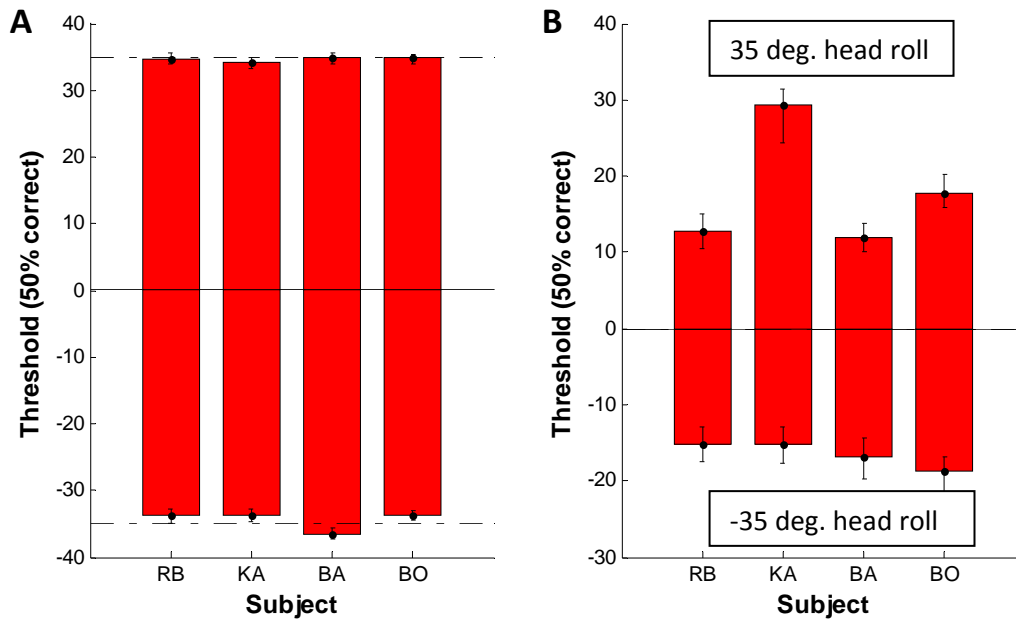


Figure 3.4. A: Threshold accuracy of all subjects. Dashed lines are the expected locations of the auditory zenith when the task is to align it with the head axis. All subjects are able to determine the location of the auditory zenith *accurately*. B: Error in threshold accuracy of all subjects when the task is to align auditory zenith with gravity axis. All subjects make significant mistakes in determining the location of the gravity axis (underestimation conform the A-effect in visual targets).

### Precision

Figure 3.5 shows the *precision* of all four subjects indicated by the slopes of psychometric curves. The first bar is the condition in which the subjects was sitting upright and had to determine whether the sound is left or right of the auditory zenith – head axis. The second and third bar are the slopes of the curves during head roll of 35 degrees, when the subject had to determine whether the sound is left or right of the gravity axis. The slopes in the latter two conditions are about the same in all subjects, but smaller than the slope of the first bar. This indicates that subjects were less *precise* when the head is tilted to a certain angle. To tell something about the dependency of precision on the head roll angle, more angles have to be investigated.

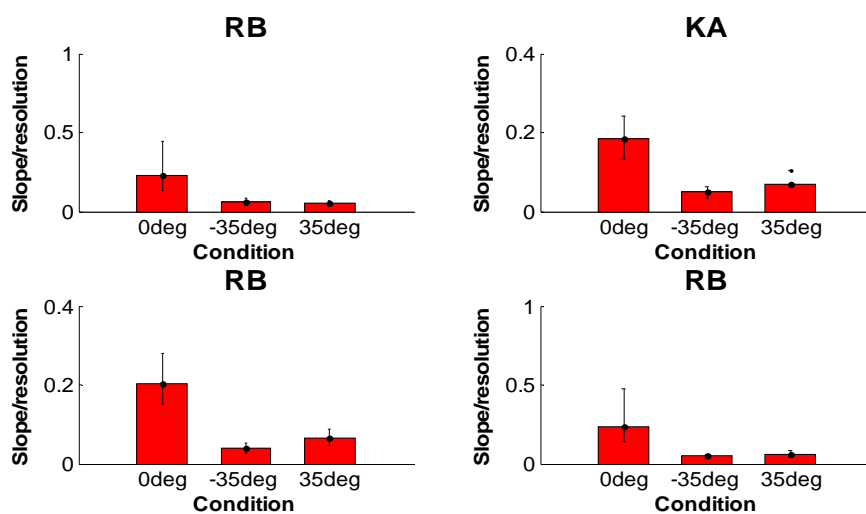


Figure 3.5. Slopes of the psychometric curves of all subject plotted against the condition. The first bar is when the subject is sitting upright and has to determine where the auditory zenith is located. The second and third bar are slopes of curves when the subject had to align the auditory zenith with the gravity axis during head roll of 35 degrees. Slopes in the latter two conditions are worse than in the condition sitting upright, meaning that subjects are getting *less precise* when the head is tilted to a certain angle.

## 4 Discussion

### Effect of auditory cues

We tested subjects on the accuracy and precision of determining the location of the auditory zenith – the point straight above the head when sitting upright. This was tested in four conditions, namely in the frontal plane (FP), midsagittal plane (MSP) and two intermediate orientations (45 and -45 degrees). Our results show that all subjects are accurate in locating the auditory zenith, but that the precision of locating the zenith is a lot worse in the MSP than in the intermediate orientations and the FP (figure 4.1). From this we conclude that around the auditory zenith spectral cues are poorly defined. Because subjects can only rely on binaural cues in the FP, and are as precise in locating the auditory zenith in the intermediate orientations as in the FP, we conclude that subjects locate sound in the intermediate orientations predominantly on binaural cues. In future research, it would be interesting to investigate more orientations in order to show whether the resolution of hearing around the auditory zenith becomes an oval (intermediate orientations resolution is dependent on the angle, getting worse closer to the MSP) or a figure eight like shape (resolution of hearing sound is bad in MSP but in intermediate orientations close to FP).

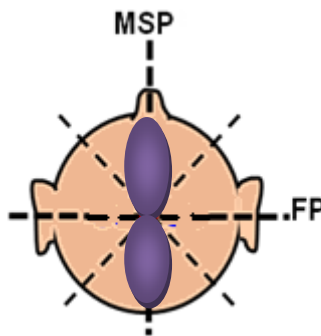


Figure 4.1. Determination of the location of the auditory zenith. In frontal plane and intermediate orientations subjects are accurate and precise in determining the location of the zenith, whereas in the midsagittal plane subjects are accurate but imprecise. This means that the resolution of hearing sound in the midsagittal plane is worse than in the other planes, indicated by the figure eight like shape.

### Auditory Aubert effect

The accuracy of determining the location of the head-centered auditory zenith during a head tilt (roll) of 35 degrees was similar as for upright (fig 3.5), but subjects were less precise.

However, when the subjects had to align the auditory zenith with the gravity axis, they were very inaccurate. Our results show an undercompensation of 30% to 80% of the roll angle, which we will call the Auditory Aubert effect. Moreover, the precision was worse for tilt than for sitting upright. This means that precision of subjects could be dependent on the angle of head roll. In order to tell more about the dependency, other angles of head roll have to be investigated too.

### Comparison to visual Aubert effect

If we compare the visual verticality perception and auditory verticality perception we can conclude that the results are qualitatively the same, but quantitatively different. The Auditory Aubert effect resembles the visual Aubert effect (Aubert, 1861; Kaptein and Van Gisbergen, 2004), although it is even larger: SVV errors are significant for angles of head roll beyond 60 degrees, whereas here we showed an error of 15 degrees at a head roll angle of already 35 deg.

### Implications for models

The De Vrijer model (2008, see Introduction) as such cannot explain the large Auditory Aubert effect. The model explains the visual Aubert-effect (A-effect is an underestimation..) with a prior assumption of head tilt. There is no reason to assume beforehand that the head position estimation should be different in an auditory task. Therefore a first modification of the De Vrijer model could be that the Auditory Aubert effect arises from target location estimation in the auditory system. A possibility would be to use Bayes' rule on the auditory information and add prior information on auditory targets. Thus, we need to know what the prior auditory information is. The most intuitive possibility would be a prior centered around the head axis. However, such a prior results in an overcompensation of auditory cues, which is the exact opposite of our results. If the auditory prior is uniform, which is a more likely possibility since in daily life sounds can be located everywhere, nothing will happen to the auditory input and the undercompensation cannot be explained either.

A different modification of the De Vrijer model could be to assume the vestibular prior to be *task* and *sensory* dependent. If the vestibular prior in auditory experiments is sharper than in visual experiments, it will have more effect on the head tilt estimation. Therefore, there will be underestimation at smaller roll angles in auditory experiments than in visual experiments. This is exactly what can be seen in our auditory experiments. In a head-fixed task, the prior is considered to be flat, resulting in an accurate estimate of head orientation.

In order to verify this modification of the De Vrijer model we propose the following experiment. First of all the Auditory Aubert effect has to be investigated at more roll angles. From the results of threshold accuracy (Auditory Aubert effect), we can create a view of how subjects estimate the location of auditory targets during head tilt ( $T_s$ ). From this we can determine what the shape of the prior should be that creates the Auditory Aubert effect.

## 5 Appendix A: Experimental Proposal Calibration Dual Search Coil

When dealing with auditory experiments, it is important to know the position of the subject's ears because then you know what the displacement is from the auditory zenith.

Robinson (1963) introduced a three dimensional head position recording technique, based on the use of a magnetic search coil. For human subjects, a dual-search coil was introduced. This dual coil consists of a direction coil and a torsion coil which are located perpendicular to each other. The direction coil is located in the frontal plane, whereas the torsion coil is located in the perpendicular sagittal plane. The torsion coil has the shape of an eight in order to cancel the flux measured in the frontal plane.

Head rotations can be described as rotations around three axes i.e. around the vertical axis, horizontal axis, and torsion axis. In dual coil calibration, we assume that rotations are described by Listings Law (Ferman et al. 1987), which is an extension of the Donders Law (Medendorp et al. 1999). Donders Law states that every point in space will give the same torsion of the head regardless the way the head rotated to that point. The basic idea behind Listings Law, is that the head can take a position reached from a reference position, the primary position, by a single rotation about a fixed axis in a flat plane, called Listings plane. So head rotations are not regarded as a sum of multiple rotations about the three main axes, but as a single rotation around a fixed axis called the rotation vector.

In order to compute the rotation vector, both an *in vitro* and a subsequent *in vivo* calibration are needed. The *in vitro* calibration determines the relative orientation and sensitivities of the search coil assembly, and the *in vivo* calibration measures the orientation of the coil during the experiment. In the next section, an experimental protocol is proposed, which allows one to determine the absolute 3D orientation of the dual search coil (Hess et al. 1992).

### Experimental Procedure

#### **In vitro calibration**

The *in vitro calibration* is done in a three-axis gimbal system in the centre of a magnetic field, which has the properties of table 1. The dual coil is mounted on the gimbal such that the voltage output of the direction coil is zero with axis 2 and 3 aligned with the horizontal and vertical magnetic fields. The torsion coil vector is mounted perpendicular to the direction coil vector. Rotations about the gimbal axis are described by the angles  $\psi$  (positive for clockwise rotation),  $\phi$  (positive for downward rotation) and  $\theta$  (positive for leftward rotation). The starting position, in which all the angles are set to zero, is called the reference position. The gimbal is rotated from 50 degrees to -50 degrees in steps of 10 degrees for each angle.

Table 1. Properties of the three perpendicular magnetic fields used.

		Horizontal (mV)	Vertical (mV)	Frontal (mV)
Torsion coil	Offset	499	457	644
	Gain	999	999	999
Direction coil	Offset	500	610	067
	Gain	999	999	999

The *in vitro* direction and torsion coil vectors are computed from the horizontal ( $d_s$ ,  $t_s$ ) and vertical ( $d_c$ ,  $t_c$ ) output voltages, which are assumed to be the sum of an offset voltage and a linear function of the sensitivity vector. Taking the difference of the output voltages for symmetrical orientations will give the vectors according to:

$$\begin{aligned}
d_1 &= -[dc(\varphi) - dc(-\varphi)] / 2 \sin \varphi \\
d_2 &= [dc(\psi) - dc(-\psi)] / 2 \sin \psi \\
d_3 &= [ds(-\psi) - ds(\psi)] / 2 \sin \psi \\
t_1 &= -[tc(\varphi) - tc(-\varphi)] / 2 \sin \varphi \\
t_2 &= [tc(\psi) - tc(-\psi)] / 2 \sin \psi \\
t_3 &= [ts(-\psi) - ts(\psi)] / 2 \sin \psi
\end{aligned}
\tag{8}$$

### In vivo calibration

The *in vivo calibration* is based on three general assumptions. First, the set up (magnetic fields, amplifiers etc.) is considered to not change during the calibration period. Second, the coil vectors length and relative angular orientation remain the same. Third of all, torsion is assumed not to change during the fixation of the vertically targets.

In order to determine the position of the vectors in space, a number of vertical fixations ( $\phi$ ) are introduced. The subject has to point a laser dot, which is head fixed, at the point of fixation denoted by a LED. The new direction and torsion coil vectors and offsets are computed using a singular value composition based on the following two equations:

$$\begin{aligned}
ds(\varphi) &= d_2 + dos \\
dc(\varphi) &= -d_1 \sin \varphi + d_3 \cos \varphi + doc \\
ts(\varphi) &= t_2 + tos \\
tc(\varphi) &= -t_1 \sin \varphi + t_3 \cos \varphi + toc
\end{aligned}
\tag{9}$$

Two additional horizontal gimbal measurements are taken into account to determine the new orientation of the two coil vectors. This is because the calculation of the  $d_2$  and  $t_2$  coil vectors involves a square root which can be negative or positive.

### Results

The *in vitro* calibration procedure was checked for each search coil, by computing the gimbal angles  $\psi$ ,  $\phi$ , and  $\theta$  from the output voltages of the dual search coil (figure 5.1). The computed angles of large rotation angles ( $> 30$  deg) varied more than 20%. These angles have been left out of the calibration procedure. Limited accuracy in the estimate of large rotation angles reflects possible experimental limitations. The subject may have problems with the fixation of the vertical angles, or the strength of the magnetic fields have changed due to electromagnetic coupling i.e. crosstalk. Furthermore, the magnetic field might not be homogeneous, or orthogonal.

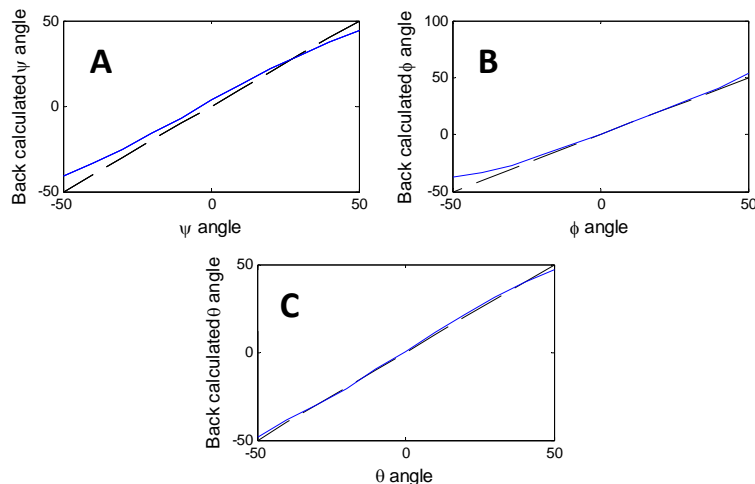


Figure 5.1. Back calculated gimbal angles from the output voltages plotted against the known gimbal angles  $\psi$ ,  $\phi$  and  $\theta$ . Note that the back calculated angles beyond 30 degrees differ a lot from the real angles.

However, the mathematical procedure is accurate when looking at the vector length (sensitivity) and the back-calculated gimbal angles. The sensitivity of the direction and torsion vector of the dual search coil, were reproducibly determined with the procedure described above to an accuracy of about 2% (table 2).

Table 2. Example of coil vector length (sensitivity), angle ( $\sigma$ ) between direction and torsion coil vector, and offset vectors after *in vitro* calibration and *in vivo* calibration.

	Vector length (mV)	Angle $\sigma$ (deg)	Horizontal Offset (mV)	Vertical Offset (mV)
<i>In vitro calibration</i>				
Direction coil	5401.1	87.6	-203.7	-3402.9
Torsion coil	906.6		-721.6	404.4
<i>In vivo calibration</i>				
Direction coil	5472.0	95.8	-558.1	-1764.5
Torsion coil	906.6		-680.1	185.3

Notice that the angle between the two vectors is different in the two calibration experiments. A possible explanation might be crosstalk (figure 5.2). If the electromagnetic coupling causes too much noise for the determination of a subject's head position, a coordinate transformation might be needed. The variables  $\alpha$ ,  $\beta$  and  $\gamma$  are chosen such that they agree with the equation

$$(9)$$

With these variables, the gimbal output voltages can be transformed into new output voltages, which in turn can be used to compute the new direction and torsion coil sensitivities.

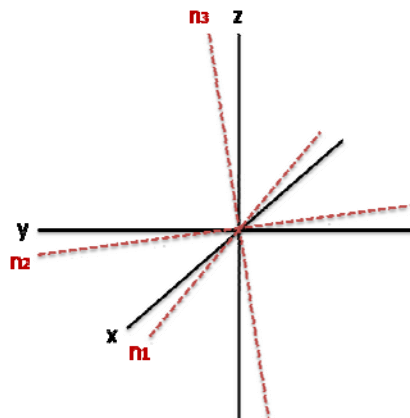


Figure 5.2. Schematic representation of crosstalk. The three magnetic fields differ in direction and strength.

## 6 Bibliography

- Angelaki, DE, McHenry, MQ, Dickman, JD, Newlands, SD, Hess, BJM (1999) Computation of Inertial Motion: Neural Strategies to Resolve Ambiguous Otolith Information. *Journal of Neuroscience* (19), 316-327
- Angelaki, DE, Dickman, JD (2000) Spatiotemporal Processing of Linear Acceleration: Primary Afferent and Central Vestibular Neuron Responses. *Journal of Neurophysiology* (84), 2113-2132
- Aubert, H (1861) Eine Scheinbare Bedeutende Drehung von Objecten bei Neigung des Kopfes nach Rechts oder Links. *Virchows Arch* (20), 381-393
- Blauert, J (1997) Spatial Hearing: The Psychophysics of Human Sound Localization. *MIT Press*
- Dayan, P, Abbot, LF (2001) Theoretical Neuroscience: Computational and Mathematical Modeling of Neural Systems. *MIT Press*, 87-88
- De Vrijer, M (2010) Multisensory Integration in Spatial Orientation, *Donders Series* (22), 57
- De Vrijer, M, Medendorp, WP, Van Gisbergen, JAM (2008) Shared Computational Mechanism for Tilt Compensation Accounts for Biased Verticality Percepts in Motion and Pattern Vision. *Journal of Neurophysiology* (99), 915-930
- Einstein, A (1908) Über das Relativitätsprinzip und die aus demselben gezogenen Folgerungen. *Jahrbuch der Radioaktivität* (4), 411-462
- Ferman, L, Collewijn, H, Van den Berg, AV (1987) A Direct Test of Listing's Law. II. Human Ocular Torsion Measured Under Dynamic Conditions. *Vision Res* (27), 939-951
- Fernandez, C, Goldberg, JM (1976) Physiology of Peripheral Neurons Innervating Otolith Organs of the Squirrel Monkey. I. Response to Static Tilts and to Long-duration Centrifugal Force. *Journal of Neurophysiology* (39), 970-984
- Hess, BJM, Van Opstal, AJ, Straumann, D, Hepp, K (1992) Calibration of Three-dimensional Eye Position using Search Coil Signals in the Rhesus Monkey. *Vision Res* (32), 1647-1654
- Highstein, SM, Fay, RR, Popper, AN (2004) The Vestibular System. *Springer*
- Jaeger, R, Kondrachuk, AJ, Haslwanter, T (2008) The Distribution of Otolith Polarization Vectors in Mammals: Comparison between Model Predictions and Single Cell Recordings. *Hear Res* (239), 12-19
- Jeffress, LA (1948) A Place Theory of Sound Localization. *Journal of Comparative Physiological Psychology* (41), 35-39
- Kaptein, RG, Van Gisbergen, JA (2004) Interpretation of a Discontinuity in the Sense of Verticality at Large Body Tilt. *Journal of Neurophysiology* (91), 2205-2214
- Medendorp, WP, Van Gisbergen, JAM, Horstink, MWIM, Gielen, CCAM (1999) Donders' Law in Torticolis. *Journal of Neurophysiology* (82), 2833-2838



- Merfeld, DM, Zupan, L, Peterka, RJ (1999) Humans use Internal Models to Estimate Gravity and Linear Acceleration. *Nature* (398), 615-618
- Middlebrooks, JC, Green, DM (1991) Sound Localization by Human Listeners. *Annual Reviews Psychology* (42), 135-159
- Mittelstaedt, H (1983) A New Solution to the Problem of the Subjective Vertical. *Naturwissenschaften* (70), 272-281
- Müller, GE (1916) Über das Aubertsche Phänomen. *Zeitschrift für Sinnesphysiologie* (49), 109-246
- Robinson, DA (1963) A Method of Measuring Eye Movement Using a Scleral Search Coil in a Magnetic Field. *IEEE Trans Biomed Eng* (10), 137-145
- Rhoades, RA, Pflanzner, RG (2001) Human Physiology, *Thomson Learning New York*
- Serway, J (2004) Physics for Scientists and Engineers with Modern Physics (6). *Thomson Learning*, 516-522
- Tollin, DJ (2003) The Lateral Superior Olive: A Functional Role in Sound Source Localization. *The Neuroscientist* (9), 127-143
- Wichmann FA, Hill, NJ (2001) The Psychometric Function I: Fitting, Sampling, and Goodness of Fit. *Perception and Psychophysics* (63), 1314-1329